Structure of Cry3A δ-Endotoxin within Phospholipid Membranes

Olga I. Loseva,‡ Elizabeth I. Tiktopulo,§ Victor D. Vasiliev,§ Alexey D. Nikulin,§ Anatoly P. Dobritsa,‡ and Sergey A. Potekhin*,§

State Research Center of Applied Microbiology, 142279 Obolensk, Moscow Region, Russia, and Institute of Protein Research, Russian Academy of Sciences, 142290 Pushchino, Moscow Region, Russia

Received January 26, 2001; Revised Manuscript Received August 31, 2001

ABSTRACT: Interaction of δ-endotoxin and its proteolytic fragments with phospholipid vesicles was studied using electron microscopy, scanning microcalorimetry, and limited proteolysis. It was shown that native protein destroys liposomes. The removal of 4 N-terminal α-helices and the extreme 56 C-terminal amino acid residues did not affect this ability. The results obtained by limited proteolysis of δ-endotoxin bound to lipid vesicles show essential conformational changes in three or four N-terminal helices and in the C-terminal region. The calorimetric method used in this study provides a unique possibility for the validation of existing models of protein binding and for a more accurate determination of the regions where conformational changes take place. It was found that the binding of the protein to model liposomes does not alter its structure in the regions starting with the fourth α-helix of domain I. This can be concluded from the fact that the activation energy of denaturation of the protein remains unchanged upon its binding to the phospholipid membranes. A new structural model has been proposed which agrees with the data obtained.

Proteinaceous crystalline inclusions are formed in *Bacillus thuringiensis* cells during sporulation. The proteins contained in these inclusions, the so-called δ-endotoxins, are toxic for insects and some other invertebrates (*1*). Based on the structure and mechanism of function, δ-endotoxins are divided into two multigenic families—Cry and Cyt (*2*). Solubilization of crystals in the midgut of insect larvae, proteolytic processing of protoxin molecules to toxins, and binding of toxins to receptors on the surface of epithelial cells and their insertion into the apical membrane generate pores that lead to distortion of osmotic balance and cell lysis (*2*−*4*).

There are data on the conformation of three Cry proteins from *B. thuringiensis*, namely, Cry3A that is active against insect larva of Coleoptera, Lepidoptera-specific Cry1Aa, and Cry2Aa with dual toxicity against lepidopteran and dipteran insects (*5*−*7*). The results obtained show that despite the differences in the amino acid sequences the proteins have a similar three-dimensional structure and consist of one α-helical (I) and two β-sheet (II and III) domains. Domain I, assumed to be pore-forming (*5*), is formed by a bundle of seven α-helical regions with a central helix α5 located inside the bundle. A similar structural motif, i.e., a "bundle" of α-helical segments with a central hydrophobic hairpin, is characteristic of some other pore-forming proteins such as colicins and B-fragment of diphtheria toxin (*8*−*12*).

Although the crystal structure of δ-endotoxins was determined and extensively studied, the conformation of pores formed by the toxin and the molecular mechanism of its insertion in membranes need to be elucidated. Insights regarding the structure of the pore-forming domain within the membrane could significantly contribute to the understanding of the mode of action of these toxins and are highly important as a paradigm for the mechanism of insertion and organization within membranes of other membrane-permeating toxins and integral membrane proteins.

Two alternative models have been proposed for the organization of the pore-forming structures of δ-endotoxin within the membrane, the "penknife" and the "umbrella" models (*5*, *13*−*15*). The same models were suggested previously for the colicin pores (*9*). The "penknife" model implies that two of the helices without significant rearrangement of the rest of domain I would flip out of domain I like a penknife opening. The "umbrella" model suggests that a pair of helices, joined to the side of domain I closest to the membrane surface, would drop down into the membrane. The remaining helices will be rearranged to be open on the membrane surface like the ribs of an umbrella. Based on the results of the interaction of synthetic polypeptides corresponding to α-helical segments of domain I with model membranes, Gazit et al. (*16*) proposed that α4 and α5 insert into the membrane as a helical hairpin in an antiparallel manner, and α7 may serve as a binding sensor to initiate structural rearrangement of this domain.

It is important that any of the models proposed for the formation of channels require partial or complete unfolding of bacterial toxin molecules for insertion of their α-helical segments into the membrane (*17*). It is evident that the conformation of the pore-forming domain can easily be changed as a result of interaction with the lipid membrane if the domain does not form a unique cooperative system. However, recently we demonstrated (*18*) that a Cry3A

* Address correspondence to this author. Phone/Fax: +7(095)924-0493, E-mail address: spot@vega.protres.ru.
‡ State Research Center of Applied Microbiology.
§ Institute of Protein Research.

10.1021/bi010171w CCC: $20.00
Published on Web 11/02/2001

molecule melts without any intermediate states and thus is a cooperative system. To elucidate this contradiction, we studied the principle of δ-endotoxin structure organization. It was shown that its structure consists of "core" and "passive" parts. By definition, the "core" involves structure elements, which undergo conformational changes when the molecule turns into the activated (or transition) state. This part of the structure is maintained due to kinetic reasons. At the same time, the structure of the "passive" part is maintained solely due to its interaction with the "core". Removal of the "passive" part evidently only slightly changes the stability of the protein, due to entropy reasons. Apparently, any change occurring in the structure of δ-endotoxin upon its binding to the phospholipid membrane should affect the thermodynamic parameters of its denaturation. If these changes involve the molecule "core", the activation energy would also change. It has an immediate impact on the half-width of the melting curves. Thus, scanning microcalorimetry provides a unique possibility to localize the range of conformational changes in a toxin molecule upon its binding to the membrane, while checking the validity of the proposed structural models of pore formation. Recently the influence of δ-endotoxin on liposomes and phase transitions in lipids forming these liposomes has been studied (*19*). The aim of this work is to elucidate changes in the structure and cooperativity of a Cry3A protein molecule during its interaction with phospholipid vesicles (liposomes).

MATERIALS AND METHODS

Isolation and Characterization of δ-Endotoxin. B. thuringiensis subsp. *tenebrionis* was grown in Ches medium (*20*) according to Mahillon and Delcour (*21*). The crystals were purified using a step sucrose gradient (67, 72, and 82%) in distilled water (*22*).

The protein concentration was determined according to Lowry et al. (*23*). Protein preparations were analyzed by polyacrylamide gel electrophoresis as described (*24*).

Determination of N-Terminal Amino Acid Sequence. After electrophoresis in SDS−PAGE, the products of proteolytic hydrolysis of Cry3A were blotted onto a poly(vinylidene difluoride) membrane (Immobilon, Millipore) in 50 mM borate buffer solution, pH 8.0, containing 20% ethanol and 0.02% β-mercaptoethanol. A Transphor 2005 (LKB) was used for electrophoretic transfer of the Cry3A fragment. Polypeptide bands were stained with Coomassie R-250 and analyzed on an automated gas-phase sequencer 477A (Applied Biosystems).

Preparation of Phospholipid Vesicles. 1-Palmitoyl-2-oleoylphosphatidylcholine (POPC), 1-palmitoyl-2-oleoylphosphatidylglycerol (POPG), and 1-palmitoyl-2-oleoylphosphatidylethanolamine (POPE) (Avanti Polar Lipids) were used. Unilamellar vesicles consisting of POPE/POPG and POPE/POPC with a molar ratio of 3:1 were prepared by reverse-phase evaporation (*25*). The required buffer solutions (glycine hydrochloride at acid pH or sodium phosphate at neutral pH) at a concentration of 25 mM were added to the mixture of lyophilized lipids. At the final stage of preparation, the samples were passed 10 times through an extruder with a 0.2 μm pore size.

Proteolysis of Protein Cry3A in the Presence of Liposomes. For proteolytic cleavage of Cry3A in the presence of phospholipid vesicles, the protein solution was intermixed with liposomes at a molar toxin-to-lipid ratio of 1:100. Hydrolysis of δ-endotoxin with trypsin or chymotrypsin in 100 mM sodium phosphate buffer, pH 7.5, was performed at the toxin-to-enzyme ratio of 1:2 at 37 °C. Samples were taken at 2, 4, and 24 h. The reaction was stopped by the addition of 2 mM phenylmethylsulfonyl fluoride (PMSF). Cry3A was cleaved with pepsin in 25 mM glycine hydrochloride buffer, pH 3.0. The protease was added at a toxin-to-enzyme ratio of 10:1. The reaction was performed at 25 °C and stopped by adjusting the pH to 8.0.

Preparation of δ-Endotoxin Fragments. To prepare a 53 kDa fragment, pepsin (Sigma) was added to δ-endotoxin in 25% methanol solution in H_2O/HCl, pH 2.0 (the toxin-to-enzyme ratio was 100:1), and the mixture was incubated at 25 °C for 4 h. The reaction was stopped by adjusting the pH to 8.0. Then the incubation mixture was dialyzed against 50 mM Tris-HCl, pH 8.0. The 53 kDa fragment that aggregates in these conditions was collected by centrifugation and dissolved in 100 mM glycine hydrochloride buffer, pH 3.0, and the protein solution was dialyzed against an appropriate buffer at 4 °C for 18 h.

To prepare a 49 kDa fragment, Cry3A crystals were dissolved in 3.3 M KBr, 50 mM sodium phosphate buffer, pH 7.0, at 37 °C for 1 h, and the insoluble material was separated by centrifugation. The supernatant was 5-fold diluted with 50 mM sodium phosphate buffer, pH 7.8. Chymotrypsin (Sigma) was added to the Cry3A solution (toxin-to-enzyme ratio was 2:1), and the mixture was incubated at 37 °C for 48 h. The reaction was stopped by the addition of PMSF to 2 mM. Then the pH of the suspension was reduced to 3.0 with 1 M HCl, and the suspension was dialyzed against 25 mM glycine hydrochloride buffer, pH 3.0. The 49 kDa fragment proved to be associated with low molecular weight polypeptides resulting from δ-endotoxin proteolysis (*26*). This complex was dissociated by incubation at 54 °C for 20 min, and the fragment was separated from the admixtures by gel chromatography on a Sephadex G-75 column (Pharmacia) at 54 °C.

Differential Scanning Calorimetry. Calorimetric measurements were made on a precision scanning microcalorimeter SCAL-1 (Scal Co. Ltd., Pushchino, Russia) with glass cells of 0.3 mL volume at a scanning rate of 1.0 K/min and an excess pressure of 2.5 atm. The protein concentration in the experiments varied from 1.0 to 3.0 mg/mL. The partial specific volumes were 0.73 cm^3/g for proteins and 0.985 cm^3/g for lipids. The excess partial heat capacity was calculated in a standard manner (*27*). A thermodynamic and kinetic analysis of the profile of the excess heat capacity was done as in Potekhin et al. (*18*).

Electron Microscopy. Mixtures of δ-endotoxin with liposomes at protein-to-phospholipid molar ratios of 1:20, 1:50, 1:100, and 1:10000 were prepared for electron microscopy analyses. The samples were negatively stained with 1% aqueous uranyl acetate using a single-layer carbon technique (*28*). Electron micrographs were taken with a JEM-100C electron microscope at an accelerating voltage of 80 kV and magnifications of 10000× and 80000×.

Bioassay. The biological activity of δ-endotoxin from Cry3A and its 53 kDa fragment was tested against the first- to second-instars larvae of the Colorado potato beetle (*Leptinotarsa decemlineata*). The proteins in 25 mM glycine

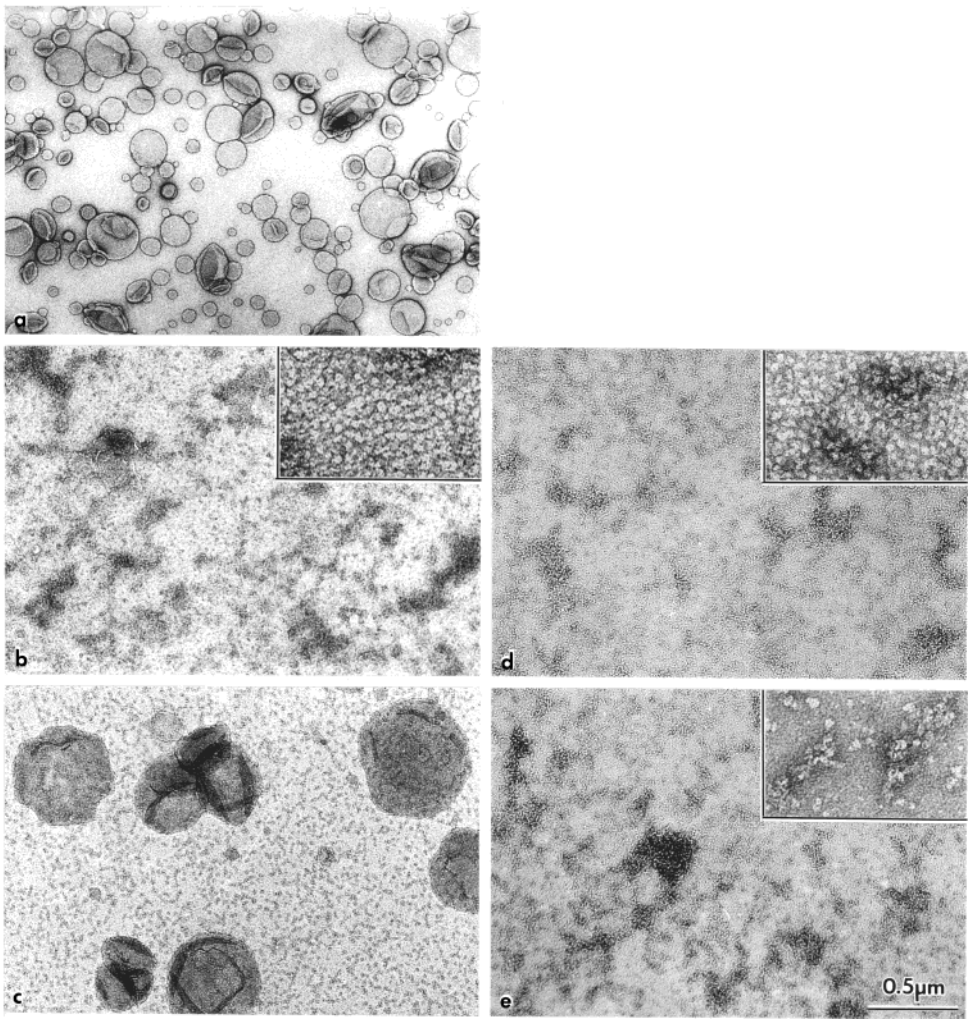

FIGURE 1: Electron micrographs of phospholipid (POPE/POPG, 3:1) vesicles before (a) and after interaction with δ-endotoxin (b, c), 53 kDa fragment (d), and 49 kDa fragment (e). Protein-to-lipid ratios are 1:50 (b), 1:100 (d, e) and 1:10 000 (c). Experiments were conducted in buffer containing 10 mM glycine hydrochloride, pH 3.0. Insets in (b, d, e) represent micrographs of the same samples at high magnification (240000×).

hydrochloride buffer, pH 3.0, were diluted in phosphate-buffered saline from 1.0 to 10^{-5} mg/mL. Potato leaves were dropped in the prepared solutions, air-dried at 20 °C, and placed in Petri dishes. Ten larvae were tested for each dilution, and 8−10 dilutions were used to determine the LC_{50} values (*29*). Mortality of the larvae was recorded after 5 days of incubation at 21 °C and a photoperiod of 18 h.

RESULTS

Electron Microscopy Analysis of Interaction of Cry3A with Liposomes. To study the effect of δ-endotoxin on model liposomes, a comparative electron microscopy examination of negatively stained phospholipid vesicles was carried out before and after the addition of δ-endotoxin (Figure 1) or its proteolytic fragments. On the electron micrographs, intact unilamellar phospholipid vesicles appear as spherical or oval bubbles of 0.02−0.2 μm (Figure 1a). An addition of δ-endotoxin leads to their destruction. When toxin-to-phospholipid molar ratios vary from 1:20 to 1:100, no vesicles are observed, and only liposome scraps and Cry3A molecules can be seen on the field of preparation (Figure 1b). These results corroborate the ability of δ-endotoxins from *B. thuringiensis* to interact with artificial lipid membranes containing no specific receptors (*30*−*32*). Moreover, Vie et al. (*33*) report results about spontaneous insertion of Cry1Aa in receptor-free lipid bilayers with the formation of pore-like structures.

Analogous processes of liposome destruction took place when liposomes were treated with the 53 and 49 kDa fragments of δ-endotoxin (Figure 1d,e, respectively). When the concentration of δ-endotoxin was reduced (the toxin-to-phospholipid ratio is 1:10 000), very large vesicles as well as aggregates of vesicles originally absent in the control sample appeared on micrographs (Figure 1c). The appearance of large vesicles suggests that the toxin can induce liposome fusion. The electron micrograph of the same preparation at high magnification is presented in Figure 2. It is clearly seen that toxin molecules are concentrated on the surface of liposomes. Moreover, in this case the surface of smooth vesicles has become rough. Similar morphological changes of vesicles obtained from the gut membranes of silkworm larvae were observed after adding the insecticidal protein from *B. thuringiensis* subsp. *kurstaki* HD-1 (*34*).

The electron microscopy data allow us to suggest the following sequence of events occurring upon the interaction of Cry3A with liposomes. If molar ratios of the toxin-to-phospholipids are low (e.g., 1:10 000), the toxin molecules, as well as some other proteins and peptides (*35*, *36*), induce

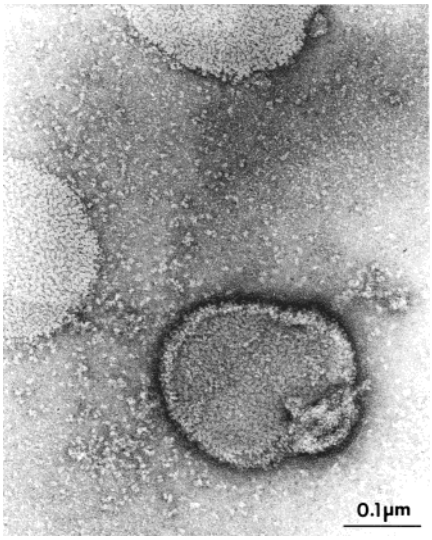

FIGURE 2: Electron micrograph of phospholipid (POPE/POPG, 3:1) vesicles in the presence of δ-endotoxin at a decreased protein-to-lipid ratio (1:10 000) and at enhanced magnification. Toxin molecules are well visible on the surface of liposomes. Experiments were performed in the same conditions as indicated in Figure 1.

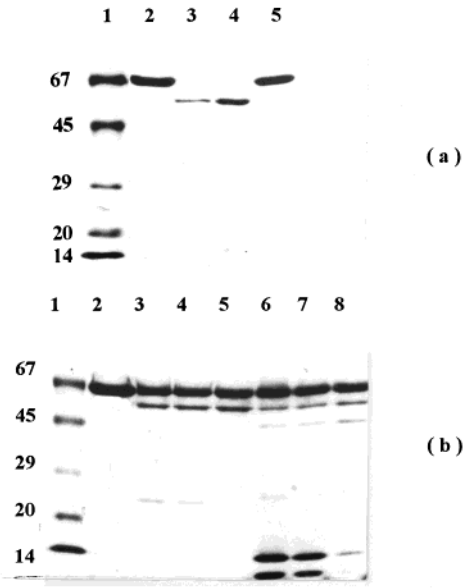

FIGURE 3: Electrophoretic analysis of Cry3A δ-endotoxin proteolytic digestion (see Materials and Methods) by pepsin (a) and by trypsin and chymotrypsin (b). In all panels, lane 1 shows marker proteins, and lane 2 shows 67 kDa δ-endotoxin. (a) Lane 3, 53 kDa fragment obtained in 25% methanol solution at pH 2.0 (3 h); lane 4, 53 kDa fragment obtained in 25 mM glycine hydrochloride buffer containing phospholipids POPE/POPC (3:1) (24 h); lane 5, proteolysis in the same conditions but without phospholipids. (b) Results of δ-endotoxin proteolysis in the presence of liposomes (2, 4, and 20 h, respectively) by trypsin (lanes 3−5) and by chymotrypsin (lanes 6−8).

fusion of liposomes into large vesicles. Moreover, it seems that Cry3A exerts a weaker effect on the integrity of small liposomes as compared to that of larger liposomes. These data indicate that binding of a relatively large number of protein molecules on the surface of any liposome is required to trigger its breakdown. Butko et al. (*37*) reported a similar result with CytA δ-endotoxin. They assumed that at least 140 CytA toxin molecules should bind to a vesicle before the latter starts losing its integrity. An increase of the concentration of δ-endotoxin induces rapid destruction of liposomes.

Thus, the results of the electron microscopy study show that, first, δ-endotoxin can bind to model liposomes in the absence of specific ligands and, second, such binding causes disruption of membranes.

Limited Proteolysis. Limited proteolysis was used to investigate changes in the structure of the Cry3A protein caused by its interaction with phospholipids.

The Cry3A protein is not practically processed upon its incubation with pepsin at pH 3.0 at least for 24 h. Nonetheless, in the presence of phospholipids or 25% methanol a 53 kDa fragment resistant to further pepsin digestion is formed (Figure 3a). The N-terminal sequence of the 53 kDa fragment is Ala-Ile-Ser-Gly-Tyr. A comparison of this sequence and the primary structure of the toxin (*38*) allows us to conclude that in this case pepsin cleaves the Phe(184)−Ala(185) peptide bond. These amino acid residues are located in the C-end of helix α4, i.e., close to the loop between the α4- and α5-helical segments in domain I (*5*).

The changes in the toxin structure caused by its interaction with phospholipid vesicles are also evidenced by the data from its treatment with trypsin and chymotrypsin. Trypsin hydrolyzes the protein in the presence of phospholipids, and the 55 kDa fragment is formed (Figure 3b). The proteolysis with chymotrypsin is more complicated: 55 and 49 kDa fragments as well as smaller peptides with molecular masses of 15 and 8 kDa are formed (Figure 3b).

Thus, the results show a remarkable acceleration of Cry3A protein proteolysis in response to its interaction with phospholipid vesicles. Based on the enzyme used, three or four N-terminal α-helices are removed. Indeed, the 55 kDa fragment formed as a result of trypsin treatment is obtained after splitting of three N-terminal α-helices (α1−α3) (*39*). The 53 kDa fragment obtained after pepsin action is a result of splitting of four α-helical segments (α1−α4). In the case of chymotrypsin processing (49 kDa fragment), 3 N-terminal α-helices (α1−α3) and 56 amino acids from the C-terminal are removed (*26*). Studies of CytA and CytB toxins from *B. thuringiensis* showed that their incubation with phospholipid liposomes also results in the appearance of new sites of protease cleavage (*40*). It is interesting that methanol can also induce certain structural changes in δ-endotoxin molecules that are similar to those occurring upon its binding to the membrane (*41*).

Effect of Lipid Bilayer on Heat Denaturation of δ-Endotoxin. As shown earlier (*18*), heat denaturation of ***δ***-endotoxin and its 55 kDa fragment are under kinetic control in solution at acid pH and can be described by a one-stage model. Thus, in addition to standard thermodynamic characteristics of denaturation, enthalpy and transition temperature, experimental data allow us to evaluate the activation energy of the rate-limited step of the process. Figure 4 shows temperature dependencies of the denaturation enthalpy and activation energy for the toxin and its fragment in solution at pH from 2.0 to 3.5 (lines 1, 2, and 5). The functions are linear and increase with a temperature increase. Earlier it was shown that the enthalpy of proteins is practically independent of solution pH and is a function of temperature only. This assumption may be also taken for the activation energy (*18*). Thus, a difference of denaturation enthalpy and activation energy for experiments at different pH reflects the temper-

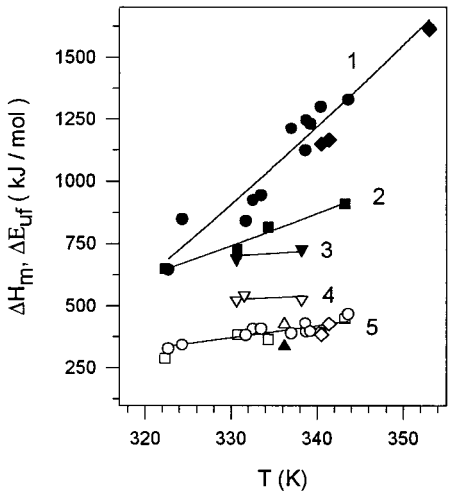

FIGURE 4: Dependence of enthalpy (filled symbols, lines 1−3) and activation energy (open symbols, lines 4−5) for denaturation versus the apparent denaturation temperature, T_m. Designations: (○,●) δ-endotoxin; (■,□) 55 kDa fragment; (▼,▽) 53 kDa fragment; (▲,△) 49 kDa fragment. Results of δ-endotoxin interaction with model liposomes are shown by (◆,◇). Straight lines are drawn by the least-squares method for every object. The data on intact δ-endotoxin in solution and the 55 kDa fragment are reproduced from Potekhin et al. (*18*). The filled diamond at ~343 K corresponds to the melting of δ-endotoxin at pH 7.4 and two different lipid contents (see Table 1).

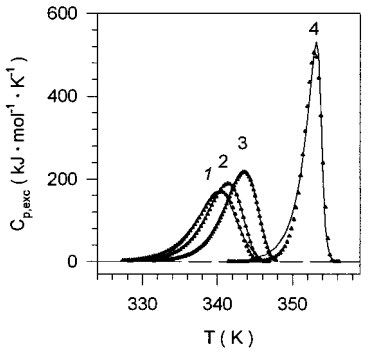

FIGURE 5: Effect of phospholipids on heat denaturation of δ-endotoxin. Temperature dependence values of the excess heat capacity functions for δ-endotoxin were obtained at pH 3.5 (curves 1−3) and 7.4 (curve 4) at a heating rate of 1 K/min. Curve 1 was obtained in the presence of liposomes containing POPE/POPG; curves 2 and 4, POPE/POPC; curve 3 was obtained in the absence of lipids. Experimental conditions are given in the legend to Table 1. The lines correspond to experimental curves. Triangles show the best fit of the experimental functions. The experimental curves of δ-endotoxin melting at pH 7.4 at two different lipid contents (see Table 1) do not differ.

ature dependence of these parameters and is not connected with any conformational alteration.

An analogous approach was used to study denaturation of δ-endotoxin bound to lipid membranes at acid and neutral pH. As seen from Figure 5, at acid pH values the curves (1−3) are in good agreement with the one-stage kinetic model. At neutral pH, the denaturation becomes more complex (curve 4) and is not a one-stage process any longer. The obtained thermodynamic and kinetic parameters of denaturation for the toxin bound to lipid vesicles are given in Table 1 and in Figure 4. It can be seen that experiments done at two different compositions of membranes produce approximately the same results. As mentioned above, the denaturation enthalpy of proteins does not actually depend

Table 1: Thermodynamic and Kinetic Characteristics of Denaturation for δ-Endotoxin and Its Fragment in the Presence and Absence of Lipids[a]

objects	pH	liposome composition	T_m (K)	ΔH_m (kJ/mol)	ΔE_{uf} (kJ/mol)
δ-endotoxin	3.0	−	338.6	1200	410
	3.5		343.6	1330	460
55 kDa fragment	3.0	−	343.3	830	470
53 kDa fragment	3.0	−	330.6	690	520
	3.5	−	338.2	730	530
49 kDa fragment	3.0	−	336.2	340	430
δ-endotoxin	3.5	POPE/POPG	340.5	1150	380
	3.5	POPE/POPG[#]	342.2	940	420
	7.4	POPE/POPG	353.0	1610	−
δ-endotoxin	3.5	POPE/POPC	341.4	1170	430
	7.4	POPE/POPC	352.9	1620	−

[a] T_m is the temperature of the peak maximum, ΔH_m is the calorimetric enthalpy, and ΔE_{uf} is the activation energy. Experiments on the influence of lipids on denaturation of δ-endotoxin were done at a protein-to-lipid ratio of 1:50. ([#]) In this experiment, the protein-to-lipid ratio was 1:20. The lipid-to-lipid ratio in liposomes was 3:1. The experiments were conducted in buffer containing 25 mM glycine hydrochloride (acid pH) and 25 mM sodium phosphate (neutral pH).

on the pH of the solution and is a temperature function. Therefore, the enthalpy values for the bound and free forms of the toxin can be compared only at the same temperature irrespective of the pH at which the data were obtained. Figure 4 shows that the denaturation enthalpies for the bound protein both at acid and at neutral pH are very close to the temperature function of denaturation enthalpy for the protein in solution (Figure 4). Usually this is interpreted as the absence of any essential conformational changes in the molecule structure (*27*). To be more exact, the change in the protein hydration during denaturation in solution and when bound to lipids is practically the same.

As for the activation energy of denaturation, Figure 4 (line 5) shows that it does not change when the protein binds to liposomes either. This means that despite direct interaction of the protein with the lipid bilayer, the kinetic pathway of protein denaturation remains unchanged. Moreover, the region of the structure determining the protein stability (the "core" of molecule) has no conformational changes upon binding as well. By definition, the "core" is the part of the structure that undergoes conformational changes upon activation of the molecule. As demonstrated earlier (*18*), this "core" does not include, at least, three N-terminal α-helices. To localize the molecule "core" more accurately, heat denaturation of two additional fragments of toxin in solution was also studied.

Heat Denaturation of 53 and 49 kDa Fragments of Cry3A Protein. The melting curves for fragments are well-described by a one-stage kinetic model of denaturation (Figure 6). The transition temperatures of the 53 and 49 kDa fragments at pH 3.0 (Table 1, Figure 6) are lower than those of intact toxin and the 55 kDa fragment (*18*). The 53 kDa fragment is less stable than the 49 kDa fragment, but its denaturation enthalpy is much higher than that of the latter (Table 1, Figure 4). Thus, cleavage of the C-terminal region decreases the denaturation enthalpy far greater than that of four N-terminal α-helices.

Figure 4 also shows that the activation energy of the 49 kDa fragment (open triangles) coincides with that of the whole molecule (line 5), whereas for the 53 kDa fragment

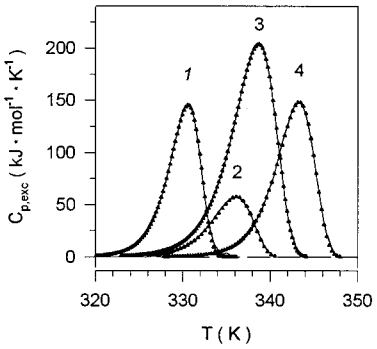

FIGURE 6: Temperature dependence of the excess heat capacity functions for δ-endotoxin (curve 3) and its 53, 49, and 55 kDa fragments (curves 1, 2, and 4, respectively) at pH 3.0 in 25 mM glycine hydrochloride buffer, and at a heating rate of 1 K/min.

it is noticeably higher (line 4). The 49 kDa fragment is 56 residues shorter from the C-end and 1 α4 helix longer from the N-end than the 53 kDa fragment. Conservation of the activation energy for a truncated protein means that the deleted region undergoes no conformational changes within the intact molecule upon activation. Therefore, it may be concluded that activation changes of δ-endotoxin structure do not occur in 3 N-terminal α-helices and in at least 56 residues from the C-end. The fourth N-terminal α-helix has already undergone conformational changes during activation and, consequently, is included in the "core" of the molecule.

It should be noted that the real experimental error in determining the enthalpy and activation energy does not exceed 10% (*27*). The scatter of experimental points (Figure 4) corroborates this. Thus, the differences in the enthalpies and activation energies for the fragments and δ-endotoxin in various states are reliable. The absence of any changes in these parameters within the limits of experimental error indicates only the absence of noticeable (large-scale) changes in the molecule structure.

Biological Tests. The insecticidal activity of the native Cry3A toxin and its 53 kDa fragment was checked on Colorado potato beetle (*Leptinotarsa decemlineata*) larvae. The LC_{50} value was 0.1 μg/mL for the intact 67 kDa Cry3A toxin and 30 μg/mL for the 53 kDa fragment. Thus, elimination of four N-terminal α-helical segments (α1−α4) reduced the toxicity of the fragment by no less than 2 orders of magnitude. Earlier it was found that proteolytic cleavage of Cry3A between α3 and α4 helices did not affect its insecticidal activity (*26, 39*).

DISCUSSION

One of the most essential results of this work is that the structure of δ-endotoxin does not change upon binding to phospholipid vesicles in the region starting with the fourth α-helix of the first domain to the 56th amino acid from the C-end. This conclusion follows directly from the fact that denaturation of the toxin bound to the lipid bilayer proceeds with the same activation energy as that of a molecule in solution (Figure 4, line 5). As shown earlier (*18*) and developed further in this paper, the molecular structure of the toxin involves both the "core" and "passive" parts. In contrast to changes in the "passive" part, any changes of the "core" structure resulting from interaction of the toxin with the lipid bilayer or from any other influence should inevitably modify the activation energy of denaturation. The available experimental data show that the "core" does not include 3 N-terminal α-helices and at least 56 amino acids in the C-terminus of the molecule. Indeed, when these regions of the structure were removed, the activation energy of the protein in solution did not change whereas the total enthalpy of the molecular denaturation was altered significantly. Additional removal of only the fourth α-helix results in an increase of the activation energy of denaturation. Thus, the fourth α-helix takes part in the activation conformational changes and is incorporated in the "core" of the molecule.

Though there were no conformational changes in the structure of the "core" of δ-endotoxin bound with phospholipid vesicles, electron microscopy data revealed its dramatic action on liposome structure. Destruction of all vesicles or at least a part of them was observed (Figure 1) in a wide range of molar toxin-to-lipid ratios (from 1:50 to 1:10 000). It should be noted that the free toxin molecules observed through the whole electron-microscopy field are hardly devoid of lipids. The fact that in the presence of lipids the calorimetric curves of toxin melting are well described by a one-stage kinetic model allows us to assert that under such conditions the toxin molecules have a unique conformation, the same for all molecules. Indeed, though in the presence and absence of lipids the difference in the denaturation transition temperatures can reach 3 °C (see Table 1, pH 3.5, POPE/POPG), an addition of lipids does not result in a more complex calorimetric curve, which should inevitably occur in the case of heterogeneity of the states of the toxin molecules.

Our conclusion on the absence of conformational changes in the larger part of the first pore-forming domain upon its binding with the membrane conflicts with the "umbrella" model. This hypothesis suggests changes of the structure practically in the whole domain I (*5, 14, 15*). In principle, our result agrees with the "penknife" model, if it is assumed that the α2−α3 helices play the role of the "blade". However, it was shown (*39*) that elimination of the first three helices has almost no affect on toxicity. Therefore, these helices and their interaction with the membrane do not play the leading role in realization of the toxic function. It is interesting that the 53 and 49 kDa fragments without several N-terminal α-helices exert a similar destructive effect on liposomes, as does the intact δ-endotoxin. If the same mechanism is valid for fragments and for intact protein, obviously, all of them have structure elements necessary for interaction with the hydrophobic core of the bilayer membrane boundaries. On the other hand, it is clear that for this type of interaction, surfaces of all these objects should have identical (or similar) hydrophobic regions, responsible for binding, with dimensions corresponding to the thickness of the hydrophobic core of the bilayer membrane (i.e., about 3 nm). However, the existing crystal structures of Cry proteins have no such region on the surface. Consequently, this region may appear only as a result of a conformational transition induced by its interaction with the membrane. This seems to be very likely, especially because α3−α4 helices become more accessible for protease action. On the other hand, our results show that such changes in the pore-forming domain can involve only three N-terminal α-helices. Thus, a significant moment here, as a result of deviation of α1−α3 helices from the rest of the protein structure, is that the hydrophobic surfaces formed by hydrophobic residues of the fourth, fifth, and seventh

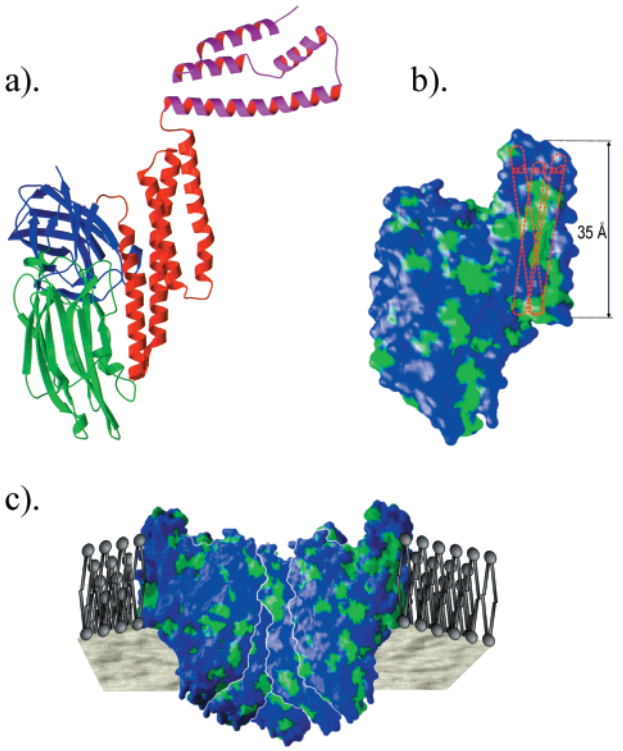

FIGURE 7: Model of interaction of Cry3A δ-endotoxin with a lipid membrane. (a) Scheme of Cry3A three-dimensional structure with three N-terminal α-helices flipped out. Domains I, II, and III are shown in red, green, and blue, respectively. (b) Molecular surface of the toxin without α1−α3 helices. The hydrophobic regions of the surface are shown in green. The projections of the three omitted α-helices are shown as cylinders. (c) Schematic representation of δ-endotoxin interaction with the lipid membrane. Helices α1−α3 in the structure of δ-endotoxin are not shown.

helices are turned open (Figure 7a). This assumption is corroborated by the reported data (*32*), which show that the enhanced membrane-perturbing activity of Cry1C δ-endotoxin at low pH correlates with the increased hydrophobic surface of the molecule. In so doing, the previous CD study demonstrated only small pH-dependent changes in the secondary structure of the proteins belonging to the Cry family (*42*).

Hence, a model that would reflect the results reported herein should take into account the following basic particulars. (i) The structure of δ-endotoxin starting with the fourth α-helix of domain I does not change upon protein binding to the membrane. (ii) The lack of three or four N-terminal α-helices of δ-endotoxin does not lead to a loss of its basic structural elements responsible for the destructive effect on the vesicles. (iii) The changes in the structure of δ-endotoxin induced by membrane−protein interaction reveal a hydrophobic region responsible for its binding with the hydrophobic core of a bilayer membrane.

A reasonable model satisfying all our data consists of the following. At the first stages of binding, three N-terminal α-helices move away from the main structure (Figure 7a), interacting with the membrane surface. As shown earlier (*16*), the second and third helices have high affinity to the membrane and are preferably oriented nearly parallel to the membrane surface. As a result of such conformational changes, the hydrophobic groups of the fifth, seventh, and fourth helices are opened (Figure 7b) which allows them to interact with the hydrophobic core of the membrane boundary. The linear dimension of the protein revealed that the hydrophobic surface is about 30 Å, which corresponds to the thickness of the hydrophobic core of a bilayer membrane. Our data do not exclude that only the first two helices move away at the first stage of binding and the hydrophobic groups of the α5 and α7 helices only form the hydrophobic surface that contacts the membrane core. However, biological tests show that the 53 kDa fragment, lacking four N-terminal α-helices, is much less active than intact toxin. Apparently, the hydrophobic residues of the α4 helix should be involved in interaction with the membrane for the toxic activity in vivo to be revealed completely. The removal of the fourth helix depresses the toxic effect of the protein but preserves its ability to interact with lipid membranes. Thus, according to this model, most of the toxin molecule inserts into the membrane, forming the channel. The outer surface of the channel is formed by hydrophobic regions of α4, α5, and α7 helices, and its lumen is lined by the hydrophilic residues of domains II and III (Figure 7c).

It should be underlined that the model in which the greater part of the toxin molecule is imbeded in the membrane is not new. Aronson et al. (*43*, *44*) have made such a conclusion using the data on treating the membrane-embedded δ-endotoxins with proteinase K. The important role of the fourth (*45*), seventh (*46*), and fifth α-helices for the toxic function was demonstrated earlier. On the other hand, the direct participation of domain III in realizing the ion channel function was also reported in a series of papers (*47*−*49*). However the proposed model does not completely agree with the data of Arnold et al. (*50*), who have demonstrated a remarkable effect of mutations in the second α-helix of domain I on the ion transport ability and the toxicity of the Cry1Ab protein. But despite the significance of the changes made (the highly conserved proline residue was altered), the toxicity dropped by no more than 3 times. Such small alterations can be caused by the indirect effect of a particular mutation. The authors believe that "the Pro70-caused broken-helix motif does seem to have a role in the topological organization of the ion channel in the larval midgut membranes".

It has been shown (Figure 1c) that Cry3A is able to induce liposome fusion at rather low concentrations when liposomes are not practically destroyed. It is known that amphiphilic helices can often induce liposome fusion (*35*, *36*), destabilizing the bilayer. It is possible that namely the interaction of the second and/or third amphiphilic helices with the membrane induces liposome fusion and facilitates embedding of the molecule into the hydrophobic core of the membrane.

Special attention should be paid to principally different contributions of C- and N-terminal parts of the Cry3A molecule to the total heat of its melting. It is obvious that removal of C-terminal amino acids leads to a sharp drop of the denaturation enthalpy of the molecule (Figure 4, Table 1). This means that interaction of this region with the "core" of the molecule will intensify with a temperature decrease. A quite different situation is observed for N-terminal α-helices. The plots of the dependence of the denaturation enthalpy of an intact molecule (Figure 4, line 1) and two fragments (lines 2 and 3) intersect at about 323 K (∼50 °C). This indicates that the contribution of N-terminal α-helices to the total enthalpy of melting is close to zero in this temperature range. At a lower temperature, their contribution

becomes negative, and the process of their separation from the "core" is endothermic. Hence, a curious and possibly important physiological conclusion can be drawn. The strength of interaction of N-terminal α-helices with the rest molecule structure is maximal at about 50 °C. The interaction diminishes with an increase and a decrease of temperature. This may be a reason for the absence of toxin action on warm-blooded animals. The process of separation of N-terminal helices from the rest of the molecule needed for embedding Cry3A into the membrane proceeds at lower temperatures.

The results of limited proteolysis of δ-endotoxin in the presence of different agents, which can somehow diminish intramolecular interactions stabilizing the protein structure, are also evidence for a rather weak interaction of these helices with the rest of the molecule at room temperature. It should be noted that protein Cry3A is not practically cleaved upon its incubation with pepsin. However, in the presence of 20−25% methanol or liposomes, the 53 kDa fragment is formed (*41*). The use of KBr or liposomes and trypsin as a protease results in the formation of a 55 kDa fragment (*18*, *39*). It is evident that the changes in the structure caused by addition of these agents increase the accessibility of proteases to the third and fourth helices, which is in good agreement with the model proposed. The results of proteolysis show that similar changes also occur in the molecule upon its binding to the membrane. Treatment with proteases can cause removal of three or four N-terminal α-helices and the C-terminal region. The physiological role of the conformational changes in the C-terminal part of the molecule is not yet clear. It may serve to fix the molecule on the membrane surface or promote the interaction between toxin molecules upon pore formation. It was shown, however, that domain III may also be involved in receptor recognition and can change insect specificity (*51*, *52*). Additional studies are required to clarify the role of this region.

ACKNOWLEDGMENT

We are grateful to Dr. T. A. Muranova for determination of the N-terminal amino acid sequence and to Dr. A. N. Naumov for determination of insecticidal activity.

REFERENCES

1. Feitelson, J. S., Payne, I., and Kim, L. (1992) *Bio/Technology 10*, 271−275.
2. Schneff, E., Crickmore, N., Van Rie, J., Lereclus, D., Baum, J., Feitelson, J., Zeigler, D. R., and Dean, D. H. (1998) *Microbiol. Mol. Biol. Rev. 62*, 775−806.
3. Hoefte, H., and Whiteley, H. R. (1989) *Microbiol. Rev. 53*, 242−255.
4. Gill, S. S., Cowles, E. A., and Pietrantonio, P. V. (1992) *Annu. Rev. Entomol. 37*, 615−636.
5. Li, J., Carrol, J., and Ellar, D. J. (1991) *Nature 353*, 815−821.
6. Grochulski, P., Masson, L., Borisova, S., Pusztai-Carey, M., Schwartz, J.-L., Brousseau, R., and Cygler, M. (1995) *J. Mol. Biol. 254*, 447−464.
7. Morse, R. J., Powell, G., Ramalingam, V., Yamamoto, T., and Stroud, R. M. (1998) *Proceedings of the VIIIth International Colloquium on Invertebrate Pathology and Microbial Control and the IVth International Conference on Bacillus thuringiensis*, Sapporo, Japan, pp 1, 2.
8. Choe, S., Bennett, M. J., Fujii, G., Curmi, P. M. G., Kantardjieff, A., Collier, R. J., and Eisenberg, D. (1992) *Nature 357*, 216−222.
9. Parker, M. W., and Pattus, F. (1993) *Trends Biochem. Sci. 18*, 391−395.
10. Wiener, M., Freymann, D., Ghosh, P., and Stroud, R. M. (1997) *Nature 385*, 461−464.
11. Elkins, P., Bunker, A., Cramer, W. A., and Stauffacher, C. V. (1997) *Structure 5*, 443−458.
12. Gouaux, E. (1997) *Curr. Opin. Struct. Biol. 7*, 566−573.
13. Hodgman, T. C., and Ellar, D. J. (1990) *DNA Sequence 1*, 97−106.
14. Knowles, B. H. (1994) *Adv. Insect Physiol. 24*, 275−308.
15. Gazit, E., and Shai, Y. (1995) *J. Biol. Chem. 270*, 2571−2578.
16. Gazit, E., Rocca, P., Sansom, M. S. P., and Shai, Y. (1998) *Proc. Natl. Acad. Sci. U.S.A. 95*, 2289−2294.
17. London, E. (1992) *Mol. Microbiol. 6*, 3277−3282.
18. Potekhin, S. A., Loseva, O. I., Tiktopulo, E. I., and Dobritsa, A. P. (1999) *Biochemistry 38*, 4121−4127.
19. Tiktopulo, E. I., Loseva, O. I., Vasiliev, V. D., Dobritsa, A. P., and Potekhin, S. A. (2000) *Mol. Biol. (Russia) 34*, 113−119.
20. Chestukhina, G. G., Zalunin, I. A., Kostina, L. I., Kotova, T. S., Kattrukha, S. P., and Stepanov, V. M. (1980) *Biochem. J. 187*, 457−465.
21. Mahillon, J., and Delcour, J. (1984) *Microbiol. Methods 3*, 69−76.
22. Thomas, W. E., and Ellar, D. J. (1983) *J. Cell Sci. 60*, 181−197.
23. Lowry, O. H., Rosenbrough, N. J., Farr, A. L., and Randall, R. J. (1951) *J. Biol. Chem. 193*, 265−275.
24. Laemmli, U. K. (1970) *Nature 227*, 680−685.
25. Szoka, F., and Papahadjopoulos, D. (1978) *Proc. Natl. Acad. Sci. U.S.A. 75*, 4194−4198.
26. Carroll, J., Convents, D., Van Damme, J., Boets, A., Van Rie, J., and Ellar, D. J. (1997) *J. Invertebr. Pathol. 70*, 41−49.
27. Privalov, P. L., and Potekhin, S. A. (1986) *Methods Enzymol. 131*, 1−51.
28. Valentine, R. S., Shapiro, B. M., and Stadtman, E. R. (1968) *Biochemistry 7*, 2143-2152.
29. Ashmarin, I. P., and Vorobiev, A. A. (1962) Statistic methods in microbiology studies (in Russian). Meditsina, Leningrad, p 182.
30. Yunovitz, H., and Yawetz, A. (1988) *FEBS Lett. 230*, 105−108.
31. Schwartz, J.-L., Garneau, L., Savaria, D., Masson, L., Brousseau, R., and Rousseau, E. (1993) *J. Membr. Biol. 132*, 53−62.
32. Butko, P., Cournoyer, M., Pusztai-Carey, M., and Surewicz, W. K. (1994) *FEBS Lett. 340*, 89−92.
33. Vie, V., Van Mau, N., Pomarede, P., Dance, C., Schwartz, J. L., Laprade, R., Frutos, R., Rang, C., Masson, L., Heitz, F., and Le Grimellec, C. (2001) *J. Membr. Biol. 180*, 195−203.
34. Tojo, A. (1986) *Appl. Environ. Microbiol. 51*, 630−633.
35. White, J. M. (1992) *Science 258*, 917−924.
36. Jahn, R., and Sudhof, T. C. (1999) *Annu. Rev. Biochem. 68*, 863−911.
37. Butko, P., Huang, F., Pusztai-Carey, M., and Surewicz, W. K. (1996) *Biochemistry 35*, 11355−11360.
38. Hoefte, H., Seurinck, J., Van Houtven, A., and Vaeck, M. (1987) *Nucleic Acids Res. 15*, 7183.
39. Carroll, J., Li, J., and Ellar, D. J. (1989) *Biochem. J. 261*, 99−105.
40. Du, J., Knowles, B. H., Li, J., and Ellar, D. J. (1999) *Biochem. J. 338*, 185−193.
41. Loseva, O. I., Tiktopulo, E. I., Dobritsa, A. P., and Potekhin, S. A. (2000) *Mol. Biol. (Russia) 34*, 123−129.
42. Venugopal, M. G., Wolfersberger, M. G., and Wallace, B. A. (1992) *Biochim. Biophys. Acta 1159*, 185−192.
43. Aronson, A. I., Geng, C., and Wu, L. (1999) *Appl. Environ. Microbiol. 65*, 2503−2507.
44. Aronson, A. I. (2000) *Appl. Environ. Microbiol. 66*, 4568−4570.
45. Masson, L., Tabashnik, B. E., Liu, Y.-B., Brousseau, R., and Schwartz, J.-L. (1999) *J. Biol. Chem. 274*, 31996−32000.
46. Alcantara, E. P., Alzate, O., Lee, M. K., Curtiss, A., and Dean, D. H. (2001) *Biochemistry 40*, 2540−2547.

47. Chen, X. J., Lee, M. K., and Dean, D. H. (1993) *Proc. Natl. Acad. Sci. U.S.A. 90*, 9041−9045.
48. Wolfersberger, M. G., Chen, X. J., and Dean, D. H. (1996) *Appl. Environ. Microbiol. 62*, 279−282.
49. Schwartz, J. L., Potvin, L., Chen, X. J., Brousseau, R., Laprade, R., and Dean, D. H (1997) *Appl. Environ. Microbiol. 63*, 3978−3984.
50. Arnold, S., Curtiss, A., Dean, D. H., and Alzate, O. (2001) *FEBS Lett. 490*, 70−74.
51. Bosch, D., Schipper, B., van der Kleij, H., de Maagd, R. A., and Stiekema, W. J. (1994) *Bio/Technology 12*, 915−919.
52. Masson, L., Mazza, A., Gringorten, L., Baines, D., Aneliunas, V., and Brousseau, R. (1994) *Mol. Microbiol. 14*, 851−860.

BI010171W